

Analysis of Load Distribution in Planet Gear Bearings

Louis Mignot, Loic Bonnard and Vincent Abousleiman

(Printed with permission of the copyright holder, the American Gear Manufacturers Association, 1001 N. Fairfax Street, Fifth Floor, Alexandria, Virginia 22314. Statements presented in this paper are those of the author(s) and may not represent the position or opinion of the American Gear Manufacturers Association.)

Management Summary

In epicyclic gear sets designed for aeronautical applications, planet gears are generally supported by spherical roller bearings with the bearing outer race integral to the gear hub. This article presents a new method to compute roller load distribution in such bearings where the outer ring can't be considered rigid. Based on the well-known Harris method, a modified formulation enables accounting for the centrifugal effects due to planet carrier rotation and the assessment of roller loads at any position throughout the rotation cycle. New model load distribution predictions show discrepancies with results presented by Harris, but are well-correlated with 1-D and 3-D finite element models (FEMs). These results validate the use of simplified, analytical models to assess the roller load distribution, rather than the more time-consuming FEMs. The results of centrifugal effects due to planet carrier rotation on roller loads are also analyzed. Finally, the impact of the positions of the rollers relative to the gear mesh forces on the load distribution is shown.

Introduction

Epicyclic gear sets are power transmission systems that provide high capacity, power density and efficiency. As such, they are widely used in various aeronautical applications, including helicopter main gearboxes and turboprop-power gearboxes, where weight is a critical performance criterion. In planetary and epicyclic gearboxes, high loads are transmitted via the planet carrier, which could result in misaligned contacts on gear meshes or planet bearings. Conventional gearbox designs thus include spherical roller bearings to support the planets on the planet carrier axles. These bearings can cope with misalignment angles up to 1.5° (Ref. 1) while providing good radial load-carrying capacity. A past study (Ref. 2) shows that bearings are a major source of failure in epicyclic gear sets. The authors also demonstrated that the optimization of planet bearings design can provide significant weight reduction, since the saving obtained on one planet is multiplied by the number of planets, which is generally greater than four. At the early gearbox design phase, it is thus essential to perform parametric studies in order to find the most optimized design for the planet bearings. Spherical roller bearings in aeronautical, epicyclic gear sets are characterized by two main features:

1. For weight-saving reasons, the outer ring of these spherical roller bearings is usually integral to the planet gear hub, which is, in addition, made as thin as possible. The gear mesh forces induced by the sun planet and the ring planet

meshes are thus applied directly to the outer ring at localized points. The conventional assumption of rigid bearing outer ring submitted to a concentrated load is not valid in this instance. The outer ring must be considered deformable to determine the roller load distribution.

2. In epicyclic gear sets, the carrier is rotating while the ring is stationary (Fig. 1). This renders the planet bearings' kinematics rather complex, with the inner ring rotating around the gearbox main axis while the outer ring is rotating around the inner ring (planet carrier axle). The effect of the centrifugal loads induced by the outer ring weight could influence the roller load distribution, since the ratio of centrifugal loads to accumulated radial gear loads can be as high as 20% for typical turboprop applications.

In this regard, several studies have been conducted to determine the influence of a deformable outer ring on the bearing loading. An analytical approach was proposed in 1963 by Jones and Harris (Ref. 3) and also described in Harris (Ref. 4). The results showed that the outer race distortion modifies significantly the roller load distribution, compared with rigid outer race assumption; i.e., the number of loaded rollers increases and the most loaded roller is no longer located along the gear tangential direction but close to mesh force application. Effects of the bearing's diametral and out-of-round clearance were also obtained with the same model by Harris et al. (Ref. 5). For this model, however, no finite element (FE) validation exists that could provide a rea-

sonable approximation of the performance of the model.

Liu and Chiu (Ref. 6) proposed a model that accounts for inertial effects induced by planet carrier rotation and roller centrifugal forces. The main results showed the influence of the bearing diametric clearance on roller load distribution and fatigue life. Some discrepancies were also observed by the authors, as compared to the Jones/Harris study (Ref. 3). Other authors have proposed an FEM approach as well; Drago et al. (Ref. 7) studied the effect of planet bearing outer race deformation on gear stresses using a 3-D FEM. The authors demonstrated that the optimization of roller loads can adversely affect gear stresses and that the planet bearing can't be designed without accounting for them.

The model presented in this article is based on the Jones/Harris approach (Ref. 3).

Initially, an example of the Jones/Harris model will be offered. A comparison of predicted loads and deformations with 1-D and 3-D FEMs will show discrepancies that can be explained by the assumptions made in the Jones/Harris equations.

Next, a new model is proposed that can solve non-symmetric problems to account for centrifugal effects due to planet carrier rotation. The results analyze the effects of centrifugal forces. The influence of roller positions with respect to mesh loads is also studied.

Analysis of State-of-the-Art Model

Jones/Harris analytical model description. In the Jones/Harris approach, the outer ring flexibility is modeled as a thin elastic ring with a mean radius R and a section moment of inertia I (Fig. 1). The effect of gear teeth on ring stiffness is ignored. The loads acting on the bearing outer ring are simplified as two equal and diametrically opposed loads representing, respectively, sun planet and ring gear planet meshes (Fig. 2). The mesh loads are assumed to act along the line of action and on the pitch radius R_p .

These loads can be decomposed into elementary radial (F_s) and tangential (F_t) forces, and a moment (M) acting on the elastic ring mean radius R . The rollers are assumed to be equally spaced around the outer ring, with the first roller located along the O-x axis defined in Figure 3. The position of the roller number j is characterized by an angle ψ_j and the reaction force of this roller on the outer ring is noted Q_j . In summary, the planet gear outer ring is submitted to mesh forces F_s , F_t , M and roller contact loads Q_j .

The system studied is thus symmetric around the O-x axis. This makes it impossible to study the influence of centrifugal effects that introduce an asymmetric force acting along the O-y axis, or to study the load distribution with arbitrary roller positions. The radial elastic ring deflection at point i —due to a load P —is expressed by means of influence coefficients C_i^P for which detailed expressions are not given in this paper but can be found in References 3–4.

$$u_i^P = C_i^P P \quad (1)$$

It is worth noting that the elastic ring deflection only takes into account the bending in the ring—excluding the

tension or shear. The validity of this approximation for rings such as the planet gears will be illustrated later in this paper. The total radial displacement at any location i is thus obtained by combining the effects of all elementary loads which yields:

$$u_i = u_0 \cos(\psi_i) + C_i^{F_s} F_s + C_i^M M + \sum_j |C_{ij}^{Q_j}| \{Q_j\} \quad (2)$$

continued

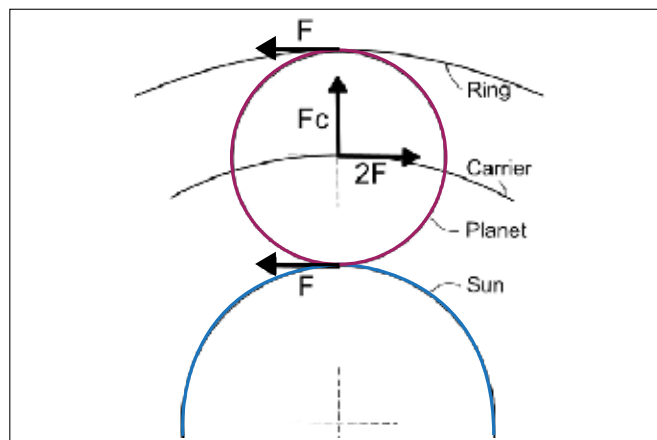


Figure 1—Loads acting on a planet.

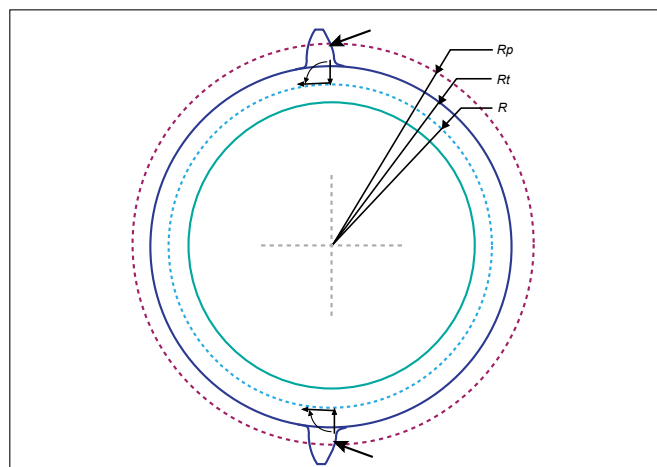


Figure 2—Simplification of mesh loads.

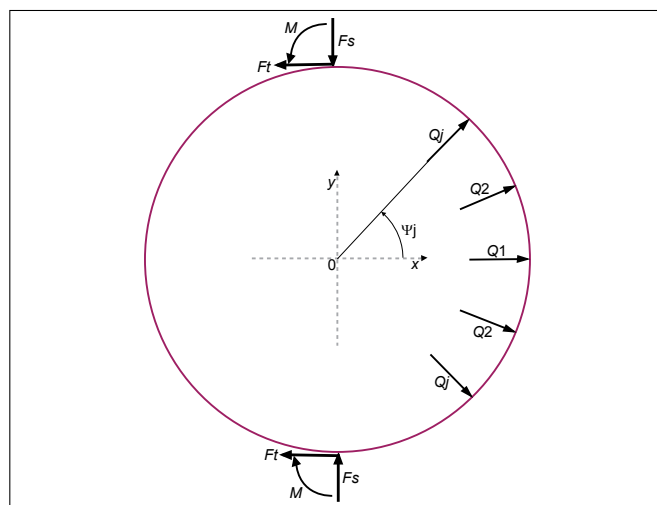


Figure 3—Forces acting on the planet gear outer ring.

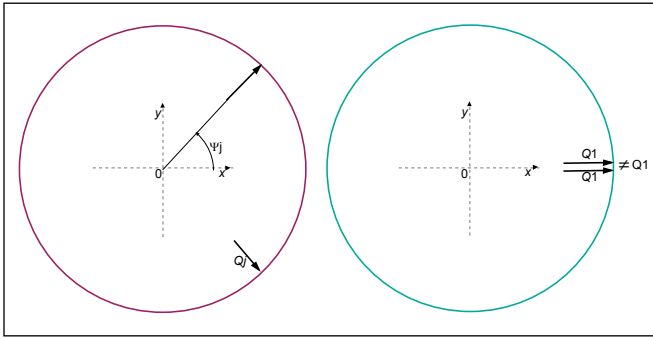


Figure 4—Jones/Harris model assumption of symmetric roller loads.

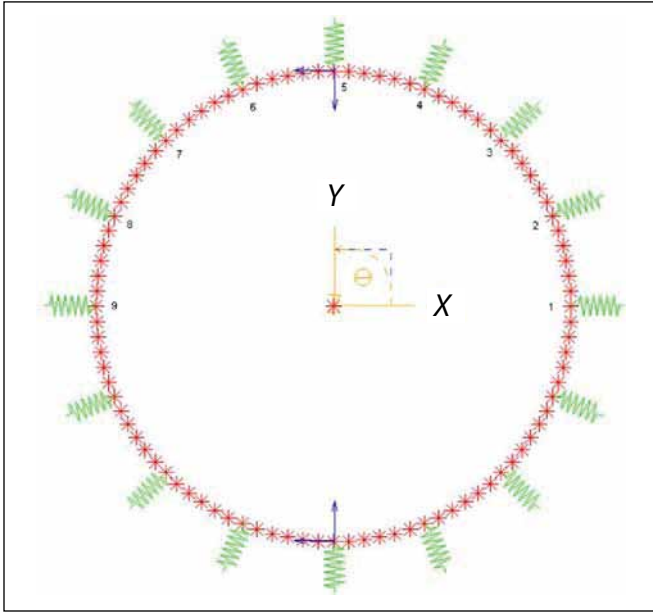


Figure 5—Example of 1-D-beam FEM.

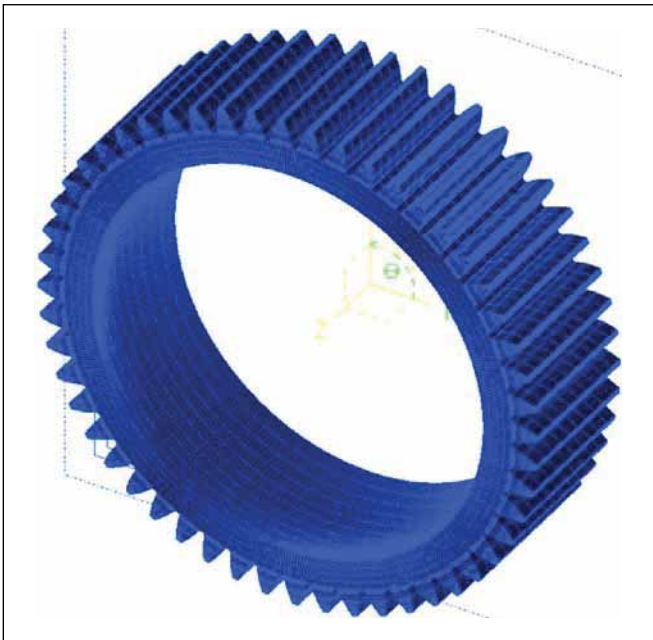


Figure 6—Example of 3-D FEM.

Using the Lundberg/Palmgren relationship, a contact condition can be defined at any roller j as:

$$Q_j = 0 \quad \text{if} \quad \left(u_j - \frac{P_d}{2}\right) \leq 0 \quad (3)$$

$$Q_j = K \left(u_j - \frac{P_d}{2}\right)^b \quad \text{if} \quad \left(u_j - \frac{P_d}{2}\right) > 0$$

Where P_d is the diametral clearance; $b = 3/2$ for point contacts and $b = 10/9$ for line contacts.

Combining Equations 2 and 3 and writing the force equilibrium along the O-x axis yields the following system of $N + 1$ equations, where N is the number of rollers:

$$u_i - u_0 \cos(\psi_i) - C_i^{Fs} F_s - C_i^M M - K \sum_j [C_{ij}^{Qj}] \left\{ \left(u_j - \frac{P_d}{2}\right)^b \right\} = 0 \quad : \epsilon_i \quad (4)$$

$$F_t - K \sum_j \tau_j \left(u_j - \frac{P_d}{2}\right)^b \cos(\psi_i) = 0 \quad : \epsilon_0$$

With,

$$\begin{aligned} \tau_j &= 0.5 \quad \text{for} \quad \psi_j = 0^\circ \quad \text{or} \quad \psi_j = 180^\circ \\ \tau_j &= 1 \quad \text{in all other cases} \end{aligned}$$

As suggested by the authors (Refs. 3–4), the non-linear system can suitably be solved by using the iterative Newton Raphson method (*Ed.'s note: the "Newton-Raphson" method is a root-finding algorithm that uses the first few terms of the Taylor series of a function $f(x)$ in the vicinity of a suspected root. A "Taylor series," developed by nineteenth-century mathematician Brook Taylor, is an infinite sum giving the value of a function $f(z)$ in the neighborhood of a point a in terms of the derivatives of the function evaluated at a .*

Remarks on the model formulae. In the Jones/Harris model, the symmetric system is solved on a half ring. Therefore, the τ_j coefficients were introduced in the force equilibrium equation (ϵ_0) to take into account half of the loads at roller positions $\psi_j = 0^\circ$ and $\psi_j = 180^\circ$; i.e., solving:

$$F_t - \frac{Q_1}{2} - Q_2 \cos(\psi_2) - \dots - Q_j \cos(\psi_j) = 0 \quad (5)$$

In displacements equations (ϵ_i), the displacement at any point i of the ring is calculated by considering a pair of roller loads Q_j symmetric with respect to the O-x axis (Fig. 4-a). It follows that when the effect of the force of Roller 1 is taken into account, it should be divided by two and not considered a pair of loads Q_1 , as shown in Figure 4-b.

A modified system of equations is proposed to solve this problem by introducing the coefficient τ_j in the term:

$$K \sum_j [C_{ij}^{Qj}] \left\{ \left(u_j - \frac{P_d}{2}\right)^b \right\} \quad (6)$$

It yields:

$$\begin{cases} u_i - u_0 \cos(\psi_i) - C_i^{Fs} F_s - C_i^M M \\ - K \sum_j \tau_j [C_{ij}^{Oj}] \left(u_j - \frac{P_d}{2} \right)^b = 0 : \varepsilon_i \\ F_t - K \sum_j \tau_j \left(u_j - \frac{P_d}{2} \right)^b \cos(\psi_i) = 0 : \varepsilon_0 \end{cases} \quad (7)$$

With,

$$\begin{aligned} \tau_j &= 0.5 \text{ for } \psi_j = 0^\circ \text{ or } \psi_j = 180^\circ \\ \tau_j &= 1 \text{ in all other cases} \end{aligned}$$

Comparison of analytical models to FEM. Two different FEMs have been built in order to validate the results obtained with the initial Harris model and the proposed, modified analytical model.

The first FEM uses one-dimensional finite elements (Fig. 5):

- The ring is modeled as an assembly of beam elements accounting for tension, bending and shear effects.
- The roller contacts are modeled as non-linear springs with a force-deflection relationship introduced via tabulated data following the Lundberg/Palmgren contact deflection law. This force deflection law accounts for the diametric clearance of the bearing (Eq. 3).

The second FEM uses 3-D (Ref. 3) finite elements (Fig. 6):

- The ring is meshed with 3-D linear hexahedric and pentahedric elements.
- The roller contact force deflection is described in the same way as in the previous 1-D FEM. In addition, rigid body elements connect the outer race nodes to each roller spring in order to distribute the contact load along the race width.
- The gear mesh loads are assumed to be uniformly distributed across the gear width.

The example used in this article is based on the data presented in Table 1.

Figure 7 displays the roller loads for the initial Harris model, the 1-D and 3-D FEM, and the modified Harris model according to Equation 5. The abscissa represents the roller number according to convention given in Figure 2. The plots show good correlation between the 1-D FEM and the modified Harris model for all rollers, whereas the initial Harris model predicts a significantly lower contact load for Roller 1 and higher loads for the other rollers. This result confirms that the missing term in the Jones/Harris model has a strong influence on the roller load distribution and must be taken into account.

The agreement between the 1-D FEM and the modified, analytical model also confirms that neglecting the tension and shear effects in the elastic ring deflection formula of the Harris analytical model is a valid assumption.

Finally, the plot in Figure 7 shows that the roller load distribution given by the 3-D FEM is similar to that of the 1-D FEM and the modified Harris model. In this case, the contact loads are greater, but are distributed on a smaller number of rollers since Rollers 5 and 9 are not loaded for

the 3-D FEM. These small differences demonstrate that the impact of tooth stiffness and 3-D effects do not play a significant role in the load distribution.

Figure 8 illustrates the ring radial displacement for the modified analytical model and the 1-D and 3-D FEMs. The FEM results appear to be in agreement, while the predicted displacements differ significantly from the analytical model. The area of greatest difference corresponds to the unloaded zone of the bearing (Rollers 6–8)—which explains why there is no impact on the load distribution, as observed in Figure 7.

These differences are believed to be a consequence of the effects of tension and shear, which are not taken into account in the analytical model.

The effect of how the gear mesh force is applied to the model has been investigated; the 3-D FEM has been run for two configurations:

- The reference model considers the gear mesh force as unique, applied at the gear pitch diameter and along the line of action.
- The second model accounts for the actual load application points on the different teeth in contact. In this case (Fig. 9), the contact is assumed to be distributed on three teeth (HCR gears).

continued

Table 1—Sample Data	
Number of rollers per row	12
Number of rows	1
Roller diameter	12.5 mm
Roller length	40 mm
Bearing clearance	0 mm
Roller contact angle	0°
Outer ring section moment of inertia	3,081 mm ⁴
Radius of outer ring neutral axis	70.3 mm
Gear pitch radius	79.5 mm
Gear mesh tangential force	27,096 N
Gear mesh separation force	9,862 N
Gear moment	249,372 N-mm

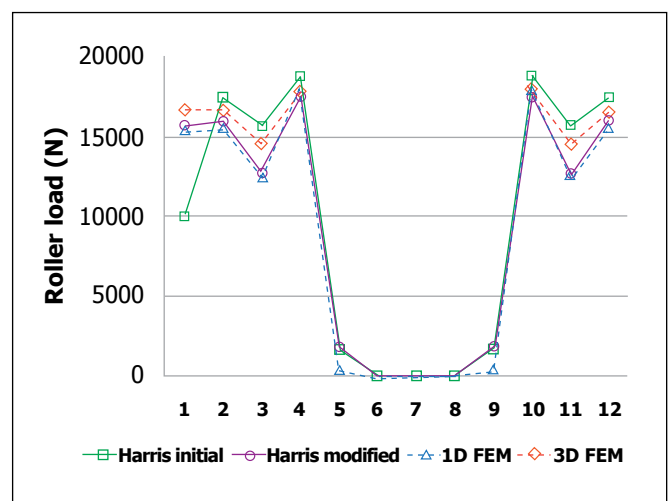


Figure 7—Roller load distribution for several models.

Figure 10 shows that the roller load distribution obtained with both models is very similar. A precise description of the tooth load distribution on the planet gear is thus not necessary as far as the assessment of the roller load distribution is

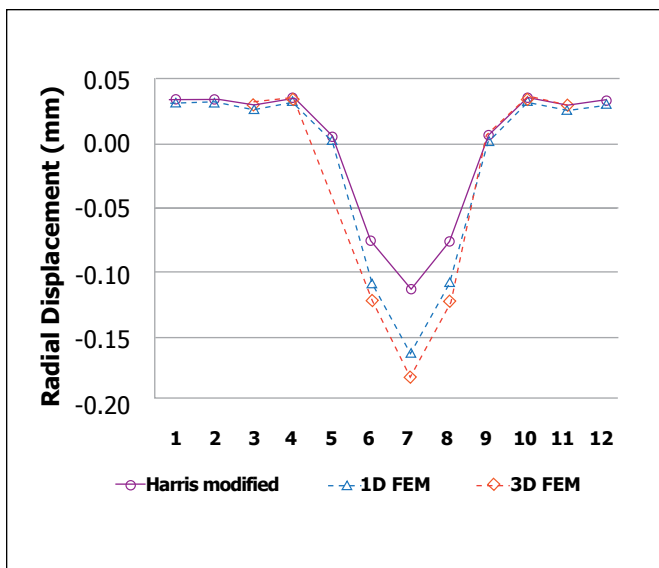


Figure 8—Ring radial displacement for several models.

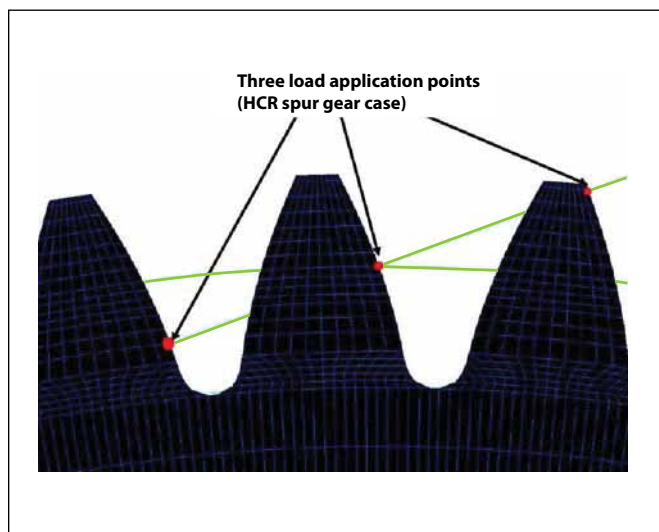


Figure 9—Influence of the gear mesh force application.

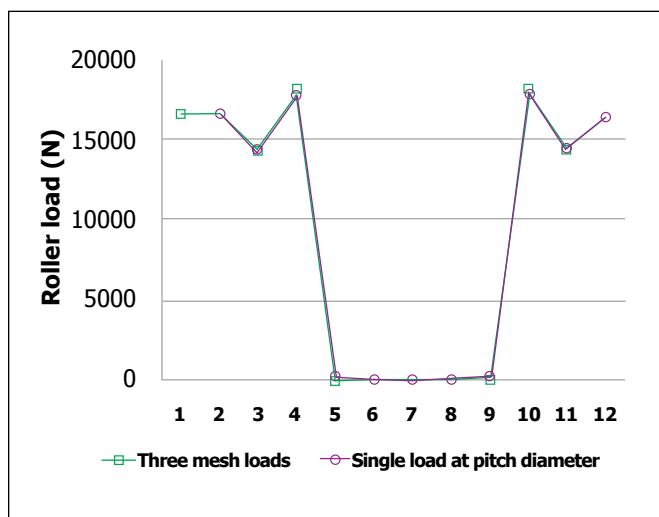


Figure 10—Roller load distribution for several models.

concerned.

The results from Figures 7–10 validate the use of a simplified analytical model in the prediction of roller load distribution. This is an important result since the analytical models can be fast to run and enable performance of parametric studies in a short time, which is not the case with 1-D or 3-D FEMs.

Improved Analytical Model

Model description. In the preceding sections, the Jones/Harris model was modified to include a missing term in the equations that appeared to be crucial in the analysis of load distribution in planet gear bearings. But this model is based on the assumption that the problem studied is symmetric about the O-x axis. This prevents, in particular:

- Accounting for the centrifugal force F_c induced by planet carrier rotation that is directed along the O-y axis. This new force will increase roller loads on the lower part of the bearing while decreasing the load on the opposite side.
- Studying the roller load distribution with an arbitrary position of the rollers with respect to the O-x, O-y axis.

The improved model presented below enables study of a dissymmetric problem by considering the roller loads Q_{jk} —not coupled symmetrically by pairs, but independent—one from the other. In order to define the radial deflection of the ring at any point i , located by the angle ψ_i and induced by a single force Q_j defined by the angle ψ_j , the influence coefficients developed by Jones/Harris (Ref. 3) for the load Q_1 were used. Indeed, these influence coefficients give the deflection at any point i due to a single load located by the angle $\psi_1 = 0$.

A local basis is created for each load application point Q_j , in which the O-x axis corresponds to the O-j direction. In this local basis, the point i_2 at which the deflection needs to be calculated is defined by an angle ψ_{i_2} (Fig. 11). In this local frame, the load Q_j is equivalent to the load Q_1 in the initial frame.

Therefore the influence coefficients given by Jones/Harris for Q_1 can be used in this basis, accounting for the relative angle ψ_{i_2} . The value of this angle is given by Figure 12 and:

$$\psi_{i_2} = \psi_i - \psi_j \quad (8)$$

Using influence coefficients of Reference 3, the deflection calculation is given by:

$$u_i^{Q_j} = \frac{1}{2} C_{i_2, j_2}^{Q_1} Q_j \quad (9)$$

Where $C_{i_2, j_2}^{Q_1}$ represents the influence coefficient defined for Q_1 (Ref. 3), but with the change of basis defined by the angle ψ_{i_2} .

Once this deflection equation is defined for the elastic ring, the system of equations can be defined as follows:

- The force equilibrium equation along the O-x axis remains the same as in the original model.
- When the planet carrier centrifugal force F_c is considered

a new equation is necessary to ensure the force equilibrium along the O-y axis. Moreover, a new rigid-body displacement u_{ob} along the O-y axis needs to be introduced.

- The equality of displacements on all ring points includes the new deflection (Eq. 9) and the contribution of the rigid body displacement u_{ob} .

It yields the following set of $N + 2$ equations:

$$\begin{cases} 2F_t - K \sum_j \left(u_j - \frac{P_d}{2}\right)^b \cos(\psi_i) = 0 & : \varepsilon_{0a} \\ -F_c - K \sum_j \left(u_j - \frac{P_d}{2}\right)^b \sin(\psi_i) = 0 & : \varepsilon_{0b} \\ u_i - u_{0a} \cos(\psi_i) - u_{0b} \sin(\psi_i) - C_i^{F_s} F_s - C_i^M M \\ - K \sum_j \left[C_{j^2, j^2} \right] \left(u_j - \frac{P_d}{2}\right)^b = 0 & : \varepsilon_j \end{cases} \quad (10)$$

Analysis of the effect of centrifugal force. The planet gear bearing defined in Table 1 is used to illustrate the effects of the centrifugal force induced by a planet carrier rotational speed of 1,500 rpm. The planet gear outer ring weight is equal to 2.38 kg and its center is located at a distance of 150 mm, relative to the planet carrier axis of rotation. In this calculation, the gear mesh forces and moment are: $F_s = 6,680$ N; $F_t = 18,553$ N; $M = 168,908$ N-mm.

Figure 13 shows a plot of the roller load distribution for the analytical model previously described in this paper, and for a 1-D FEM. Both curves are in agreement—thus validating the new analytical model.

The roller load distributions are no longer symmetric with respect to the O-x axis—i.e., Rollers 1 and 7. The rollers located at the radial outer part of the bearing (Rollers 1–6) carry a lower load than those located at the inner part of the bearing (Rollers 7–12). The difference in the maximum loads carried by each area of the bearing is equal to 18%—which is significant. The effect of centrifugal force shall therefore not be neglected in the design phase—both for the sizing to contact pressure and to the sliding in unloaded zones.

Influence of roller position relative to the gear mesh.

Due to the natural symmetry of a bearing, the system returns to an identical state at every cage rotation. In the Jones/Harris model (Ref. 3), an important assumption is that Roller 1 is by necessity located along the O-x axis—at angle $\psi_1 = 0$. Between $\psi_1 = 0$ to $\psi_1 = \frac{2\pi}{N}$ the original Jones/Harris model cannot predict the load distribution.

This new model makes possible the modeling of the different roller position configurations by introducing a shift angle in the calculation of ψ_{i2} . This possibility is illustrated in the numerical application shown in Table 2.

Figure 14 shows the roller load distribution for the initial position with an 11.43° angular shift. The main impact is seen on the rollers close to the gear mesh; i.e., Rollers 5–6 for the ring gear mesh and Rollers 13–14 for the sun gear mesh. This is due to the sudden change in the outer ring deformed shape in the vicinity of the mesh forces and

continued

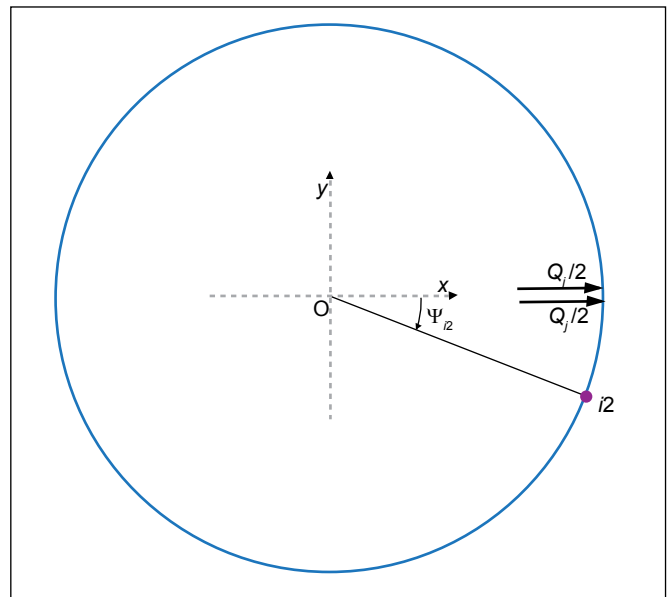


Figure 11—Definition of the local frame at Q_i .

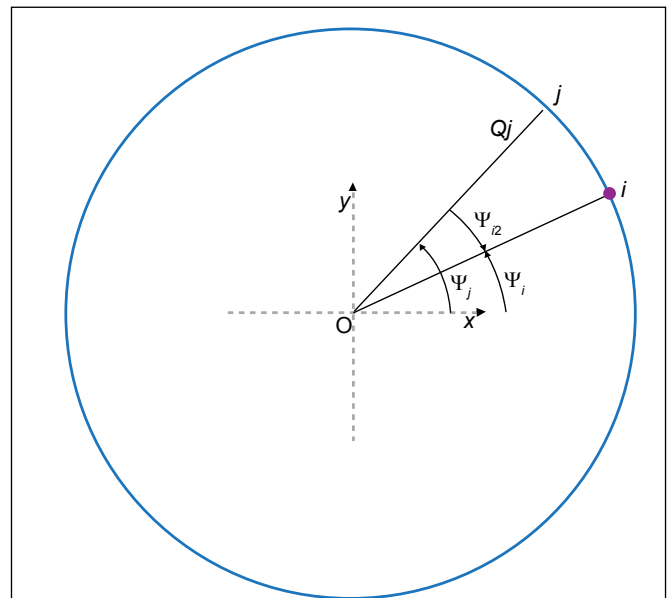


Figure 12—Change of basis definition for the improved model.

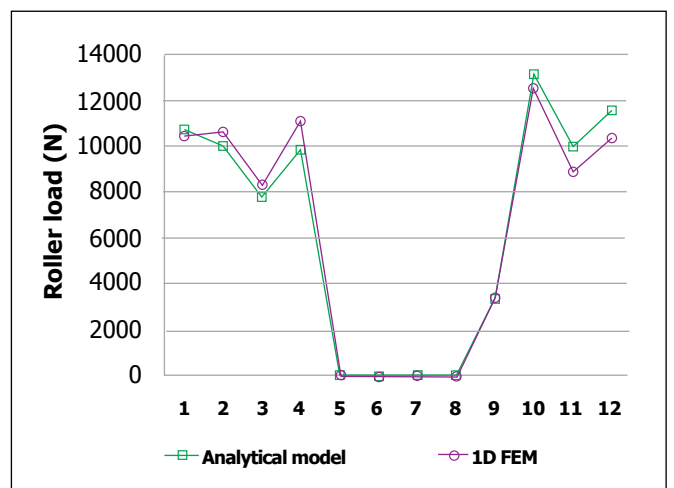



Figure 13—Effect of planet carrier rotation centrifugal force on the roller load distribution.

moment, which affects the bearing clearance and thus the contact load (Fig. 15). The consequence is a significant increase in the maximum roller load from 5,867 N to 7,689 N (+ 31%). This high roller load variation could be lowered by stiffening the outer ring.

Conclusion

In the first part of this article, a missing term in the Jones/Harris model has been identified; the corrected system of equations showed correlation with 1-D and 3-D FEMs. In particular, the practice of modeling precisely the gear teeth and the tooth load distribution has a negligible effect on the prediction of roller load distribution. The ability to use simplified, analytical models with reasonable confidence in the result is important, since designers generally need a fast tool to perform parametric studies at an early stage of the design. A limitation in the use of simplified models is the fact that they can't assess the stress state in the outer ring as precisely as do FEMs; in certain cases the stresses might be the limiting factor in the design of the outer ring.

A new model has also been presented that enables the study of dissymmetric systems—such as the ones that take into account planet carrier rotation centrifugal effects or that simulate arbitrary roller positions. Centrifugal effects tend to create asymmetric load distribution in the bearing, with a load increase in the sun gear mesh area. The position of the rollers relative to the gear mesh forces has also shown to be a critical parameter, since in this area the outer ring deformation is maximal.

The model improvements will be directed towards the integration of rollers' individual centrifugal loads that may affect the load distribution in the bearing. In addition, efforts will be made to include in the model the assessment of the planet rim stresses. This latter improvement should allow optimization of the rim thickness as a function of rim stresses and roller load distribution. 

Vincent Abousleiman is chief design engineer/power transmission division at Hispano-Suiza; Loic Bonnard is a hydraulic engines application engineer at Poclair Hydraulics and Louis Mignot is a power transmission design engineer at Eurocopter.

References

1. Hamrock, B.J. and W.J. Anderson. "Rolling-Element Bearings," NASA Reference Publication 1105, 1983.
2. Black, J.D. and E.E. Pfaffenberger. "Design of the High-Reliability GMA2100 Reduction Gearbox," 1991, American Institute of Aeronautics and Astronautics paper.
3. Jones, A.B. and T.A. Harris. "Analysis of a Rolling Element Idler Gear Bearing Having a Deformable Outer-Race Structure," *ASME Journal of Basic Engineering*, 1962, pp. 273–278.
4. Harris, T.A. *Rolling Bearing Analysis*, 4th Ed., 2001, John Wiley & Sons Inc., New York.
5. Harris, T.A. and J.L. Broschard. "Analysis of an Improved Planetary Gear Transmission Bearing," *ASME Paper No. 63-LUB-2*, 1964, pp.457–462.
6. Liu, J.Y. and Y.P. Chiu. "Analysis of a Planet Bearing in a Gear Transmission System," *ASME Paper No. 75-LUB-23*, 1976, pp. 40–46.
7. Drago, R.J. and R.N. Margasahayam. "*Stress Analysis of Planet Gears with Integral Bearings: 3-D Finite-Element Model Development and Test Validation*," Advanced Power Train Group, Boeing Vertol Company, Philadelphia, PA.

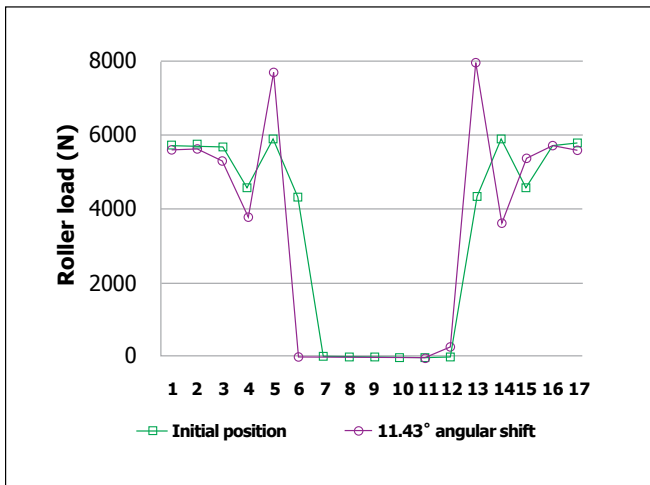


Figure 14—Effect of roller positions on the roller load distribution.

Table 2—Shift angle in the calculation of ψ_{12}	
Number of rollers per row	17
Number of rows	2
Roller diameter	16 mm
Roller length	16 mm
Bearing clearance	0.03 mm
Roller contact angle	10.9°
Outer ring section moment of inertia	2,375 mm ⁴
Radius of outer ring neutral axis	70.49 mm
Gear pitch radius	79.5 mm
Gear mesh tangential force	27,096 N
Gear mesh separation force	9,862 mm
Gear moment	244,210 mm

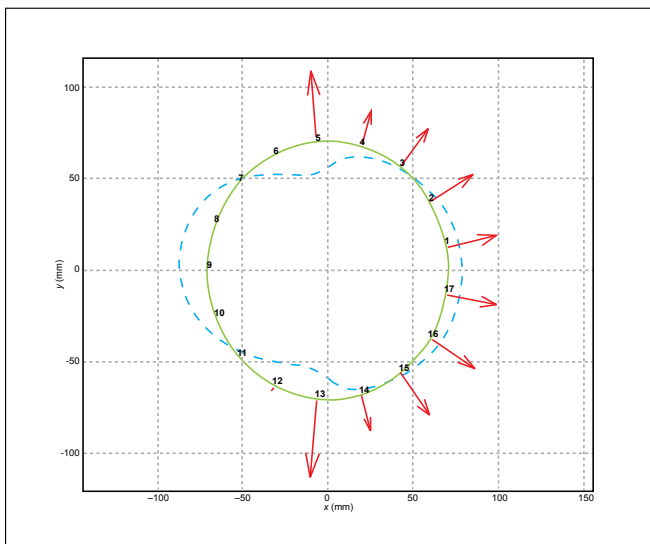


Figure 15—Outer ring—deformed shape—and corresponding roller loads.